Polymer Chemistry

Evaluating Polymerization Kinetics Using Microrheology

Journal:	*Polymer Chemistry*
Manuscript ID	PY-ART-02-2024-000188.R1
Article Type:	Paper
Date Submitted by the Author:	23-Mar-2024
Complete List of Authors:	Salas-Ambrosio, Pedro; University of California Los Angeles, Chemistry and Biochemistry Gupit, Caidric; UC Santa Barbara Uruena Vargas, Juan Manuel; UC Santa Barbara Luo, Yimin; University of California Santa Barbara, Mechanical Engineering and Materials Science Gupta, Rohini; BASF Corporation Valentine, Megan; University of California, Santa Barbara, Mechanical Engineering Maynard, Heather; University of California Los Angeles, Chemistry and Biochemistry Helgeson, Matthew; UC Santa Barbara, Chemical Engineering Hankett, Jeanne; BASF Corporation

Evaluating Polymerization Kinetics Using Microrheology

Pedro Salas-Ambrosio,[1,3†] Caidric I. Gupit,[2†] Juan Manuel Urueña,[3] Yimin Luo,[2,4‡] Jeanne M. Hankett,[5] Rohini Gupta,[6] Megan T. Valentine,[2*] Heather D. Maynard,[1,3*] Matthew E. Helgeson[4*]

[1] Department of Chemistry and Biochemistry and California Nano Systems Institute, University of California Los Angeles, Los Angeles, CA, USA

[2] Department of Mechanical Engineering, University of California Santa Barbara, Santa Barbara, CA, USA

[3] BioPACIFIC Materials Innovation Platform, California Nano Systems Institute, University of California Santa Barbara, Santa Barbara, CA, USA

[4] Department of Chemical Engineering, University of California Santa Barbara, Santa Barbara, CA, USA

[5] BASF Corporation, Wyandotte, MI, USA

[6] BASF Corporation, California Research Alliance (CARA), Berkeley, CA, USA

† Equal contribution

‡ Current Address: Department of Mechanical Engineering and Materials Science, Yale University, New Haven, CT, USA

* Corresponding author

Electronic supplementary information (ESI) available: Table S1; Figures S1–S14.

Abstract

Monitoring the kinetic evolution of the molecular weight of a growing polymer is critical to understand and optimize polymerization reactions for materials development and discovery. In this work, we propose the use of passive probe microrheology as a facile and low-cost method to monitor polymer growth kinetics by indirectly tracking the molecular weight evolution of a polymerizing reaction mixture using time-resolved measurements of sample viscosity. To do so, a recently developed Brownian probe microrheology method based on differential dynamic microscopy (DDM) was applied to a model system of dimethylacrylamide undergoing reversible addition-fragmentation chain-transfer (RAFT) polymerization. The polymerization rate constants extracted from microrheology were within 20% of those obtained from conventional nuclear magnetic resonance (NMR) spectroscopy and size-exclusion chromatography (SEC) measurements. A simple and intuitive workflow based on a single-point Mark-Houwink analysis was then used to estimate an apparent viscosity from NMR and SEC data and, equivalently, an apparent molecular weight from microrheology data. Over the expected range of validity of the analysis, the results are in reasonable quantitative agreement with the corresponding independently measured values. The results demonstrate the ease and reliability of inferring the molecular weight from viscosity data and highlight the capability of DDM microrheology to monitor polymerization of polymer systems.

1. Introduction

Monitoring polymerization and evaluating reaction kinetics provides fundamental understanding of polymerization chemistries, and is used to explore the performance of new polymerization chemistries. This knowledge enables optimization of reactions to produce polymers with controlled properties and consistent quality. This in turn improves efficiency, minimizes costs and emissions, and ultimately accelerates material development and discovery as well as technological applications of polymeric materials.[1] This endeavor generally involves screening a wide range of polymerization chemistries and conditions, leading to a large parameter space that is efficiently explored through high-throughput, data-driven experimentation.

In practice, polymerization is typically monitored by measuring material properties and their evolution as the reaction progresses, which include the polymer molecular weight,[2] sample viscosity,[3] and reaction conversion[4] using techniques including real time Fourier-transform infrared spectroscopy,[5] Raman spectroscopy,[6] or photo-differential scanning calorimetry.[7] Among these, the molecular weight is the most informative as it reports the degree of polymerization, and determines the mechanical properties of the resulting material, which informs its processability and performance in intended applications.[8–10] The conventional technique to measure molecular weights is size-exclusion chromatography (SEC). However, obtaining SEC measurements can require extensive sample preparation, generation of calibration standards, long data acquisition times, and use of relatively large volumes of potentially hazardous solvents.[2] When screening large parameter spaces, this can make SEC a relatively costly method to deploy between resource usage, and time and effort.

Techniques that circumvent the drawbacks of SEC while providing molecular weight information are therefore desirable. A possible alternative is to measure the polymer viscosity in solution, which depends on and, in principle, could report the polymer molecular weight.[11] A potential route for using solution viscosity measurements to estimate the molecular weight is the well-known Mark-Houwink relation, a semi-empirical model that describes the scaling of viscosity with the average molecular weight, with coefficients that have been characterized for many polymer chemistries.[12–15] While this relation has been established for extracting molecular weight from viscosity of as-prepared polymer solutions,[11] this is not the case for the kinetically evolving molecular weight of polymerizing samples since access to this information requires not only the solution viscosity but also the polymerization kinetics.

Among available techniques to measure solution viscosity and monitor polymerization kinetics, passive microrheology is particularly attractive, involving measurements of viscosity through analysis of the Brownian motion of embedded probe particles. Compared to conventional bulk-scale rheology and viscometry, microrheology offers the advantages of smaller sample volumes, relatively short data acquisition times, minimal perturbation of fragile or history-dependent samples, and access to long time scales (days to weeks) and weak moduli (as in the case of evolving and soft materials like polymer solutions), as well as opportunities to access and measure sample variation in heterogeneous

materials.[17–19] Despite these advantages, microrheology has not yet been established as a technique to monitor polymerization and evaluate polymerization kinetics because the conventional data analysis tool – multiple particle tracking – lacks the throughput necessary to perform real-time analysis of kinetic data sets.

In this work, we utilized the capability for high-throughput data acquisition and analysis with minimal need for user intervention of passive microrheology based on differential dynamic microscopy (DDM), an emerging microrheological technique with strong potential for *in situ* measurements.[20–23] An intuitive workflow is presented to estimate the molecular weight from the measured viscosity and polymerization kinetics. The results were validated against the conventional nuclear magnetic resonance (NMR) spectroscopy and SEC, and demonstrated the utility of microrheology as an attractive alternative to monitor polymerization.

2. Experimental methods

2.1. Materials

The chemicals used in this work were purchased from Sigma-Aldrich and Tokyo Chemical Industry. Dimethylacrylamide (DMA) monomer was passed through a basic aluminum oxide bed to remove the 4-methoxyphenol inhibitor, while the chain transfer agent (CTA) 2-(((butylthio)carbonothioyl)thio)propanoic acid (95%) was used as-is. Azobisisobutyronitrile (AIBN) initiator was recrystallized from acetone before use. Dimethyl sulfoxide (DMSO), deuterated DMSO (DMSO-d6), and dimethylformamide (DMF) solvents were dried using molecular sieves and kept under an inert atmosphere.

2.2. Sample preparation

The DMA monomer and the CTA in DMSO solvent were mixed in a Schlenk flask followed by the addition of the AIBN initiator also in DMSO. The mixture was degassed using a freeze-pump-thaw procedure for five cycles and was then stirred at 75 ºC. Aliquots were taken at different time points and the reaction was quenched by cooling to ambient temperature and exposing to air. To vary the rate of the reaction and the degree of polymerization, the initial DMA concentration was varied from 4.5 to 27 wt%, and the molar equivalent of DMA relative to the CTA was varied from 50 to 200, while the molar equivalent of AIBN relative to the CTA was kept constant at 0.25.

The samples measured for calibration to determine the Mark-Houwink constants were prepared in a similar way, with the following modifications. After degassing, the reaction mixture was stirred at 75 ºC for 16 h, dialyzed (molecular-weight cutoff at 1 kg/mol) against deionized water, and then freeze-dried. In these samples, the initial DMA concentration was fixed at 27 wt%, the molar equivalent of DMA relative to the CTA was varied from 50 to 500, and the molar equivalent of AIBN relative to the CTA was kept constant at 0.25. The resulting yield, degree of polymerization, number-average molecular weight, and dispersity of these polymer samples are provided in **Table S1**.

2.3. Sample characterization

2.3.1. Size-exclusion chromatography (SEC)

SEC measurements of polymers in DMF with 0.1 M lithium bromide were performed on a high-performance liquid chromatography system (1260 Infinity II, Agilent) where each sample was measured for three replicates. The chromatography system was equipped with two columns (PLgel MIXED-D, Agilent; molecular weight range of 0.2–400 kg/mol) as well as multi-angle light scattering and differential refractive index detectors (Wyatt Technology). The flow rate was 0.6 mL/min and the column temperature was held at 40 ºC. The molar mass was calculated using the refractive index increment, dn/dc, of 0.80 determined experimentally.

2.3.2. Proton nuclear magnetic resonance (^{1}H-NMR) spectroscopy

^{1}H-NMR measurements of polymers in perdeuterated DMSO were performed on a Bruker spectrometer (Bruker; 400 MHz). Each sample was measured for six replicates. The spectra were analyzed using the MestRenova v12 software.

2.3.3. Rheology

Rheological measurements of polymers in DMSO were performed using a stress-controlled rheometer (AR-G2, TA Instruments) with an upper cone geometry (60 mm diameter, 2° angle) and a lower plate geometry with a Peltier temperature controller. Each sample was measured for three replicates. The shear rate was increased from 0.1 to 100 s^{-1}, and the lower plate was maintained at 25.0 ± 0.1 °C.

2.3.4. Capillary viscometry

Viscosity measurements of polymers in DMSO were performed using an automated rolling-ball viscometer (Lovis 2000 M, Anton Paar) with a glass capillary (internal diameter of 1.8 mm) and a steel ball. Each sample was measured for three replicates. The inclination angle ranged from 20° to 55° depending on the sample viscosity, and the sample chamber was kept at 25.0 ± 0.1 °C.

2.3.5. Optical microscopy

100 µL sample aliquots were mixed with fluorescent probe particles (SPHEROTECH; polystyrene, carboxylated surface, Nile red, diameter of 0.53 µm) for a concentration of approximately 1.5×10^6 particles/µL or 0.011 vol%, prior to transferring to a 96 well-plate (Cellvis) which was then sealed with pressure-sensitive adhesive tape (Thermo Fisher Scientific). Each sample was measured for six replicates using an inverted microscope (Axio Observer 7, Zeiss) with a computer-controlled and motorized sample stage which was calibrated using the Zeiss ZEN software to automatically and successively image each well in the plate. The sample environment was maintained at 30 ºC using an incubation system. The images were captured using a 20 × objective lens (plan-apochromat, Zeiss; NA = 0.8, resolution of 0.293 µm/pixel) and a monochromatic camera (Axiocam 702, Zeiss). All samples were imaged via epifluorescence to maximize the signal-to-noise ratio, using a Colibri 7 light source and a standard DsRed filter set (excitation at 538-562 nm, emission at 570-640 nm). For each measurement of viscosity, a time series of 1000 images was recorded with a field of view of 150 × 150

μm and at a focal plane ~100 μm above the glass/sample interface, using a 50 ms exposure time and a 10 Hz frame rate.

2.3.6. Differential dynamic microscopy (DDM) microrheology

DDM analysis was performed on the recorded video images without any pre-processing of the images, as previously described.[20,21] In brief, intensity differences between successive images separated by lag time, τ, were computed, then Fourier transformed and ensemble-averaged in the wave vector, q, range of 0.042–10.701 μm^{-1} in this work to calculate the image structure function $D(q,\tau)$,

$$D(q,\tau) = A(q)[1 - f(q,\tau)] + B(q) \quad (1)$$

where $A(q)$ and $B(q)$ are related to the probe's intensity profile and the incoherent background, respectively, and $f(q,\tau)$ is the intermediate scattering function. In ergodic systems, as $\tau \to 0$ and $\tau \to \infty$, $f(q,\tau)$ is equal to 1 and 0, respectively, and thus $D(q,\tau)$ is equal to $B(q)$ and $A(q) + B(q)$, respectively, based on eq 1. For a Gaussian distribution of displacements,[20]

$$\langle \Delta r^2(\tau) \rangle = \frac{4}{q^2} \ln \left[\frac{A(q)}{A(q) + B(q) - D(q,\tau)} \right] \quad (2)$$

where $\langle \Delta r^2(\tau) \rangle$ is the mean-squared displacement.

To implement eq 2, we follow the analysis method of Gu *et al*.[21] Briefly, to improve the accuracy of the resulting $\langle \Delta r^2(\tau) \rangle$, $D(q,\tau)$ curves at q values with $\sigma/A(q) \geq 0.025$, where σ is the standard deviation of $A(q)$, were excluded from the analysis. These excluded curves typically correspond to low q-values or large length scales which are characterized by large displacements where the measurement time can be too short to adequately sample $D(q,\tau)$, and high q-values or small length scales which are characterized by small displacements and are thereby more prone to experimental uncertainty. In addition, $D(q,\tau)$ curves were truncated at τ when $D(q,\tau) > 0.8[A(q) + B(q)]$ to ensure that $A(q) + B(q) - D(q,\tau)$ does not approach a value of zero which would lead to large and divergent values of the displacement, according to eq 2.

In all cases, we observe that $\langle \Delta r^2(\tau) \rangle$ follows a linear trend with τ, from which the translational diffusion coefficient, D, was obtained, by the two-dimensional Einstein equation,

$$\langle \Delta r^2(\tau) \rangle = 4D\tau \quad (3)$$

which was then used to calculate the solution's zero-frequency viscosity, η, using the Stokes-Einstein relation assuming Brownian motion in a Newtonian fluid,

$$\eta = \frac{k_B T}{3\pi d D} \quad (4)$$

where k_B is the Boltzmann constant, T is the temperature, and d is the probe's diameter.

3. Results and discussion

In order to establish microrheology as a technique to evaluate polymerization kinetics, we sought to analyze a model (controlled) polymerization where the individual polymer chains in solution increase in molecular weight at approximately the same rate. Thus, at any instant during the polymerization, the polymer can be represented by an average molecular weight, which can be correlated with monotonic changes in the viscosity of the solution. In general, we will show that this relationship can be used to obtain kinetic parameters of an ongoing polymerization reaction. For the more specific case of reactions producing polymers with low dispersity, we will further show that this enables one to obtain direct estimates of the average molecular weight. Such a model polymerization system was achieved through the use of reversible addition-fragmentation chain-transfer (RAFT) polymerization, which is a controlled radical polymerization able to produce polymers with controlled molecular weights and low dispersity.[24]

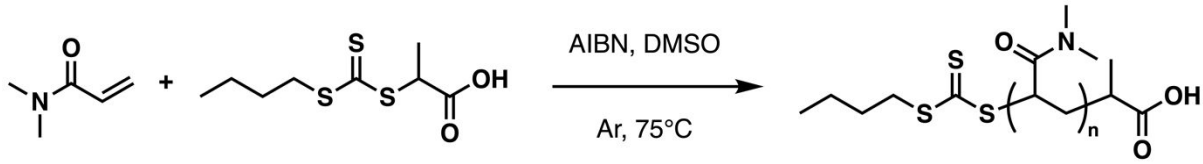

Figure 1. Reaction scheme for the reversible addition-fragmentation chain-transfer (RAFT) polymerization of dimethylacrylamide in DMSO under an argon atmosphere at 75 ºC using 2-(((butylthio)carbonothioyl)thio)propanoic acid as the chain transfer agent and azobisisobutyronitrile as the initiator.

In this study, we used RAFT polymerization to produce poly(dimethylacrylamide) (PDMA) using the scheme shown in **Figure 1**. To evaluate the kinetics of the polymerization, the rate of the reaction and the degree of polymerization were controllably varied by changing the initial concentration of the monomer, c_{m0}, and the molar equivalent of the monomer relative to the chain transfer agent, n_{eq}, respectively. DDM-based microrheology was then performed on sample aliquots collected at certain times after initiation of the polymerization and after mixing with fluorescent probe particles.

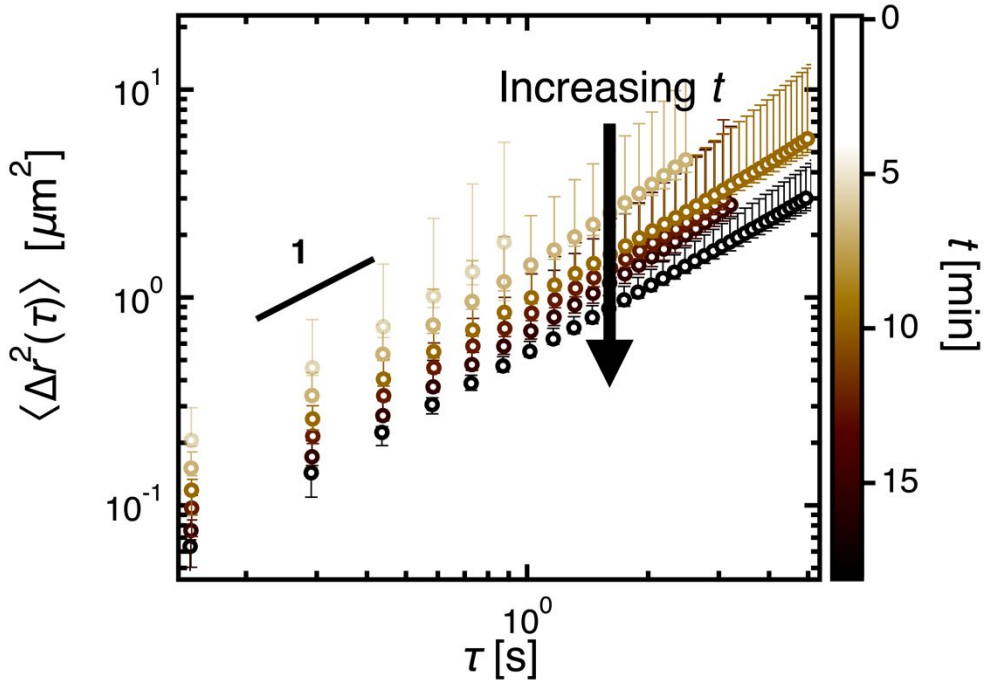

Figure 2. Mean-squared displacement, $\langle \Delta r^2(\tau) \rangle$, as a function of lag time, τ, at various reaction times, t, after initiation of the polymerization represented by the color bar. The samples were prepared at initial monomer concentration, c_{m0}, of 18 wt% and molar equivalent of monomer relative to the chain transfer agent, n_{eq}, of 50. The error bars represent standard deviations after ensemble averaging in the differential dynamic microscopy (DDM) analysis.

Using DDM, we obtained the mean-squared displacement, $\langle \Delta r^2(\tau) \rangle$, of the particles as a function of lag time, τ, at c_{m0} = 18 wt%, n_{eq} = 50, and at various times during polymerization. The determination of $\langle \Delta r^2(\tau) \rangle$ and quantification of the standard deviation was automated using a previously developed, fast, and robust analysis without the need for user input.[21]

As the polymerization proceeds, the scaling relationship $\langle \Delta r^2(\tau) \rangle \sim \tau$ with an exponent of unity was observed, indicating that the probe particle motion remained diffusive and solutions behaved as Newtonian fluids over the measured frequency range which was further confirmed using bulk rheometry (**Figure S1**).[22,25] However, across the range of τ, the measured $\langle \Delta r^2(\tau) \rangle$ continuously shifted to lower values with increasing polymerization time **(Figure 2)**. This reflects the slower motion of the probe particles due to the increase in viscosity as the polymers in solution grow. The same trends were observed using sample solutions at different c_{m0} and n_{eq} (**Figure S2**). We note that the variation in the cutoff τ value for $\langle \Delta r^2(\tau) \rangle$ at various times after polymerization initiation results from the requirement that $\langle \Delta r^2(\tau) \rangle$ be calculated at τ values where $D(q,\tau)$ is less than 80% of $A(q) + B(q)$ (eq 1).[20] At long τ, the weak upturn in $\langle \Delta r^2(\tau) \rangle$ is due to the convective drift caused by thermal gradients in the system, and the increase in standard deviation of $\langle \Delta r^2(\tau) \rangle$ is then due to the small number of displacements available which leads to poor statistics at these long lag times. If desired, access to longer values of τ could be provided by acquiring videos of probe motion over longer times.

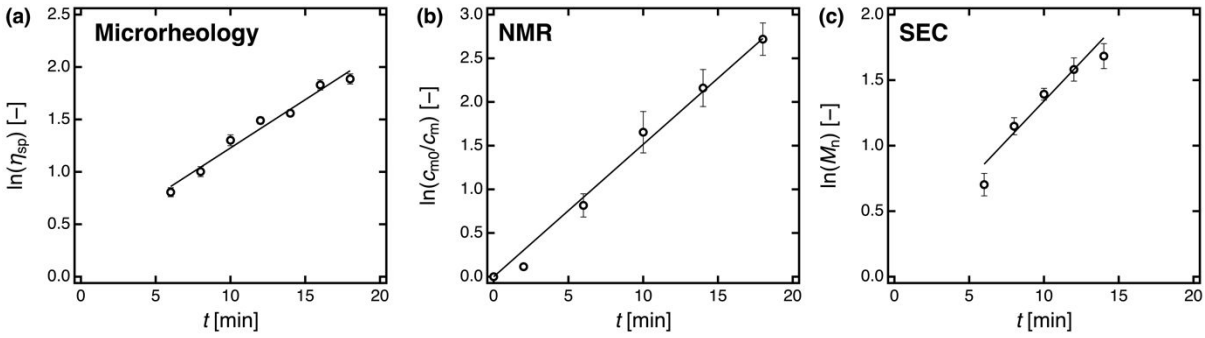

Figure 3. Dependence on the polymerization time, t, of (a) the ln of the specific viscosity, $\eta_{sp} = (\eta - \eta_s)/\eta_s$ where η and η_s are the viscosities of the solution and solvent, respectively, measured using differential dynamic microscopy (DDM)–based microrheology; (b) the ln of c_{m0}/c_m where c_{m0} and c_m are the initial and instantaneous concentrations of free monomer, respectively, measured using ^{1}H nuclear magnetic resonance (NMR) spectroscopy; and (c) the ln of the number-average molecular weight, M_n, measured using size-exclusion chromatography (SEC). All data were obtained at c_{m0} of 18 wt% and molar equivalent of monomer relative to the chain transfer agent, n_{eq}, of 50. The error bars represent standard deviations of six replicate measurements. Solid lines indicate weighted fitting based on a linear fit.

From the measured values of $\langle \Delta r^2(\tau) \rangle$ versus τ, a weighted fitting procedure taking into consideration the standard deviation of $\langle \Delta r^2(\tau) \rangle$ was used to determine the diffusion coefficient, D, (eq 3) and subsequently the solution viscosity, η, (eq 4). In cases with an upturn in $\langle \Delta r^2(\tau) \rangle$ at long τ, the additional term $v^2\tau^2$ was introduced in eq 3 to account for the convective drift with speed v. The resulting viscosities were validated against those from bulk rheometry and capillary viscometry measurements (**Figure S3**). The quantitative agreement in η between microrheology and bulk measurements using rheometry and capillary viscometry demonstrates the stability of the probe particles used in the samples without observable probe aggregation nor polymer adsorption onto the probes during the microrheology measurements. These η values were also consistent with those determined from the decay of the intermediate scattering function, $f(q,\tau)$, and were independent of the wave vector, q, as expected for a homogeneous fluid (**Figure S4**). The η was then expressed in terms of the specific viscosity, $\eta_{sp} = (\eta - \eta_s)/\eta_s$ where η_s is the viscosity of the pure solvent. When measured as a function of polymerization time, t, a monotonic increase in η_{sp} was observed as expected for growing polymers in solution over time (**Figure 3a**).

To compare the kinetics measured by microrheology to those measured by more conventional techniques, we compared the time-evolution of viscosity reported by DDM microrheology to the increase in c_{m0}/c_m, where c_m is the instantaneous concentration of free monomer measured using nuclear magnetic resonance (NMR) spectroscopy (**Figure 3b**; representative spectra in **Figure S5**), as well as the increase in the number-average molecular weight, M_n, measured using size-exclusion chromatography (SEC) (**Figure 3c**; representative chromatograms in **Figure S6**). We found qualitatively good agreement between the time course of signal increase in all three methods – i.e., all measurements produce a signal that is monotonically increasing, with an approximately exponential dependence. This indicates that DDM microrheology can sensitively detect changes in the solution

viscosity due to the growing polymer and moreover, that these changes can be used to monitor the polymerization with access to similar time scales as provided by the conventional techniques of NMR and SEC. In addition, the monotonic increase in the various polymer properties with t indicates polymerization kinetics that are independent of the instantaneous molecular weight of the growing polymer, at least within the studied range of 2.0–23.9 kg/mol. This monotonic trend further demonstrates the successful use of RAFT polymerization to provide reaction control in this case, as expected. The molecular weight dispersities, Đ, determined from SEC remained low and within the range of 1.1–1.2 during polymerization (**Figure S7**) while the final reaction conversions determined from NMR were within the range of 91–97% (**Figure S8**) at c_{m0} of 4.5–27.0 wt% and n_{eq} of 50–200.

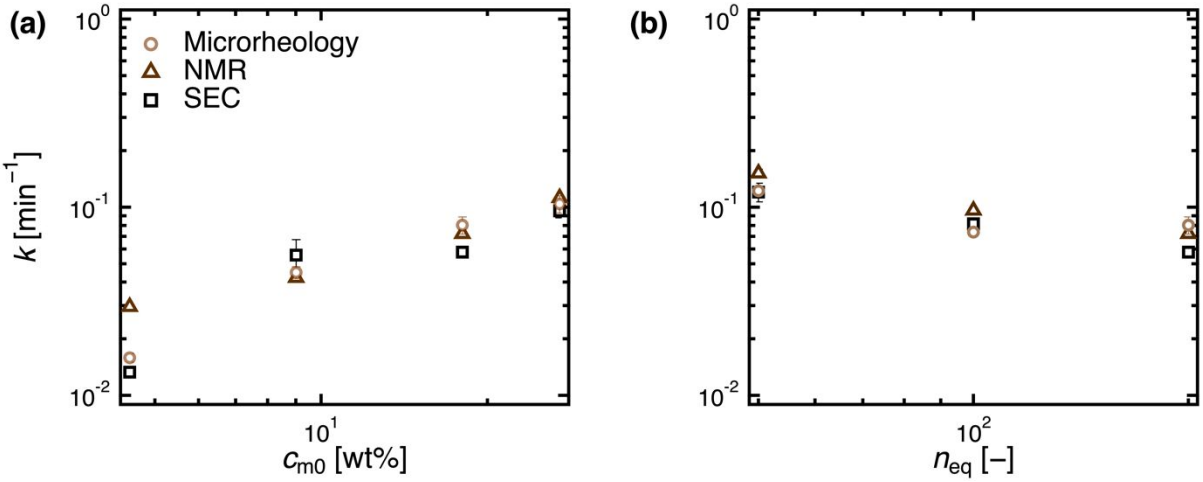

Figure 4. Rate constants, k, as functions of (a) the initial monomer concentration, c_{m0}, and (b) the molar equivalent of monomer relative to the chain transfer agent, n_{eq}, determined from differential dynamic microscopy (DDM)–based microrheology, nuclear magnetic resonance (NMR) spectroscopy, and size-exclusion chromatography (SEC). The error bars represent standard deviations of the best-fit curves (**Figures S9-S11**) which, in most cases, are smaller than the data markers themselves.

To quantitatively compare the polymerization kinetics evaluated by DDM microrheology with those by the conventional techniques of NMR and SEC, a corresponding pseudo-first order rate constant, k, was determined for each method by plotting the natural logarithm of the polymer properties against the reaction time t (**Figure 3**) and then fitting with the first-order rate equation, $\ln(\mathrm{X}) = kt$ where X refers to η_{sp} (**Figure S9**), $c_{\mathrm{m0}}/c_{\mathrm{m}}$ (**Figure S10**), or M_{n} (**Figure S11**). A pseudo-first order reaction rate was confirmed from the linear plot of $\ln(c_{\mathrm{m0}}/c_{\mathrm{m}})$ vs t and was assumed to apply to the t-dependence of η_{sp} and M_{n}. As such, the range of time points included in the fit was determined when the coefficient of determination, R^2, is above a threshold value of 0.9 (**Figures S12-S13**). **Figure 4** shows k obtained for variations of c_{m0} and n_{eq}. Quantitative agreement in k values obtained using the three techniques was observed to within 20%. This validates DDM microrheology as a viable alternative technique to monitor the characteristic rates and timescales of polymerization, providing nearly indistinguishable information as compared to conventional NMR and SEC techniques.

Further validation of DDM microrheology was performed by comparing the measured viscosity with an apparent viscosity that can be estimated from the NMR and SEC data by leveraging the known relationships between viscosity, molecular weight, and polymer concentration, as follows. We begin by considering the semi-empirical Mark-Houwink equation,[11]

$$[\eta] = KM_{\mathrm{v}}^{a} \tag{5}$$

which relates the intrinsic viscosity, $[\eta]$, which itself depends on η and the polymer concentration c, to the viscosity-averaged molecular weight, M_{v}. In this expression, K and a are the Mark-Houwink constants, which depend on the polymer/solvent pair and temperature,[11] and were determined from a double logarithmic plot of $[\eta]$ vs M_{v}. The value of M_{v} was approximated to be equal to M_{n} considering that M_{v} values typically lie between M_{n} and M_{w}, the weight-average molecular weight,[26] and in the present study, M_{w} differs with M_{n} by only a factor of 1.1–1.2 determined by the polymer dispersity, $Đ = M_{\mathrm{w}}/M_{\mathrm{n}}$ (**Figure S7**).

The value of $[\eta]$ for a particular molecular weight was estimated using the Rao-Yaseen equation,[27]

$$[\eta] = \frac{1}{2c}[\eta_{\mathrm{sp}} + \ln(\eta_{\mathrm{rel}})] \tag{6}$$

where $\eta_{\mathrm{rel}} = \eta/\eta_{\mathrm{s}}$ is the relative viscosity. Eq 6 provides a simple, fast, and accurate method to estimate $[\eta]$ from η at a single concentration c ideally in the dilute condition. This simplification was validated against the conventional and more rigorous method to determine $[\eta]$ from η at different values of c followed by extrapolation to c = 0 (**Figure S14**).

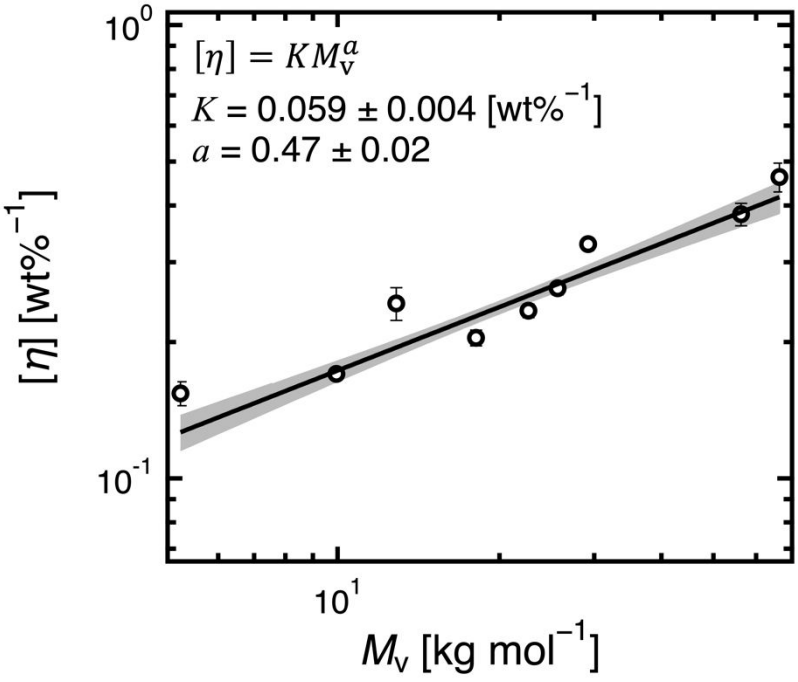

Figure 5. Intrinsic viscosity, $[\eta]$, as a function of viscosity-averaged molecular weight, M_{v}. $[\eta]$ was estimated using the Rao-Yaseen equation[27] (eq 6). The solution viscosity at 4 wt% polymer concentration was measured by differential dynamic microscopy (DDM)–based microrheology, while M_{v} was approximated by the number-averaged molecular weight, M_{n}, measured by size-exclusion chromatograph (SEC). The error bars represent standard deviations after ensemble averaging in the DDM analysis of the image series. The solid line indicates weighted fitting based on the Mark-Houwink equation (eq 5) with the shaded region indicating the 95% confidence interval of the fit and resulting Mark-Houwink constants K = 0.059 $\pm$ 0.004 (wt%$^{-1}$) and a = 0.47 $\pm$ 0.02.

A plot of $[\eta]$ as a function of M_{v} is shown in **Figure 5**, where $[\eta]$ was estimated at c = 4 wt% which is within the dilute regime and the range of validity of eq 6 (**Figure S14**). The Mark-Houwink equation (eq 5) fits the data well, with resulting Mark-Houwink constants K = 0.059 $\pm$ 0.004 (wt%$^{-1}$) and a = 0.47 $\pm$ 0.02. Using these values of K and a, as well as the measured values of c obtained from NMR and M_{n} obtained from SEC, it is possible to estimate apparent viscosity values using eqs 5-6. Note that the statistical uncertainty is propagated through this analysis and accounted for in the calculated values. These calculated apparent values were then compared with the measured viscosity values determined experimentally using DDM microrheology.

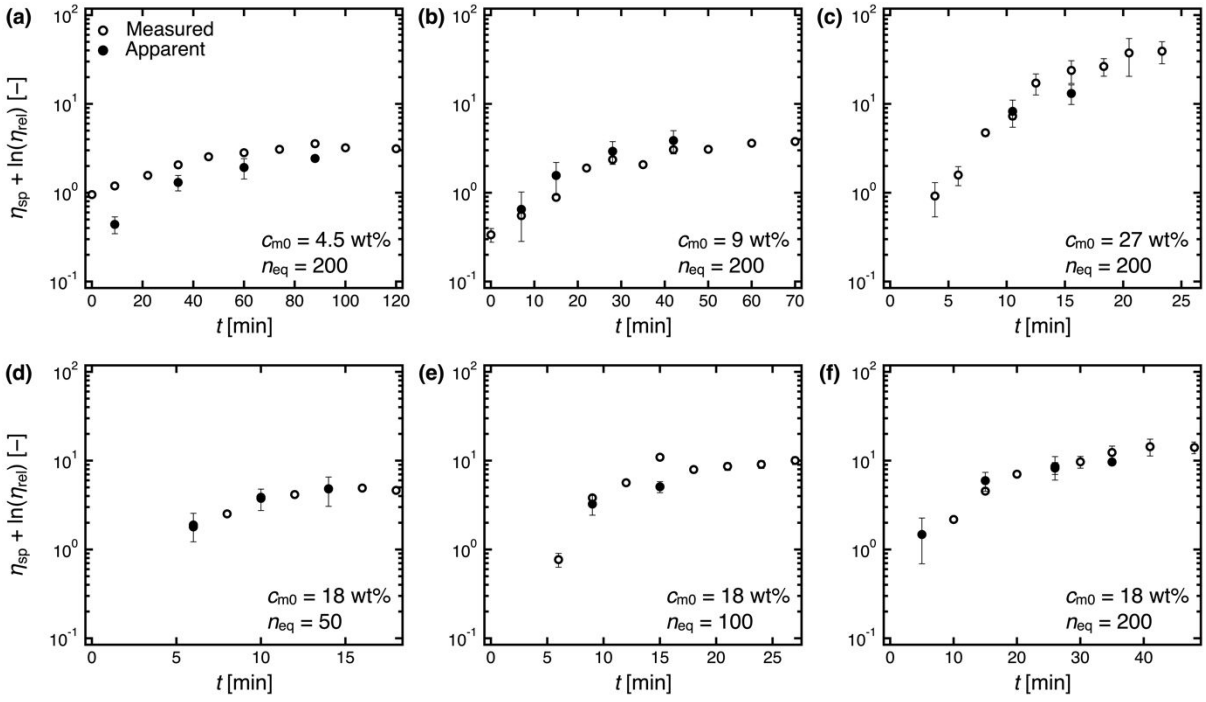

Figure 6. Comparison of measured viscosity from DDM–based microrheology (empty circles) and apparent viscosity (filled circles) estimated from NMR and SEC data as functions of polymerization time, t, at various (a–c) initial monomer concentrations, c_{m0}, and (d–f) molar equivalents of monomer relative to the chain transfer agent, n_{eq}. The viscosities are expressed as $\eta_{\mathrm{sp}} + \ln(\eta_{\mathrm{rel}})$ based on eq 6, where η_{sp} and η_{rel} are the specific and relative viscosities, respectively. The error bars represent standard deviations of six replicate measurements which, in most cases, are smaller than the data markers themselves.

Figure 6 shows the measured and apparent viscosities expressed as $\eta_{\mathrm{sp}} + \ln(\eta_{\mathrm{rel}})$ based on eq 6 as functions of polymerization time at various c_{m0} and n_{eq}. Due to the more limited time resolution involved

with the longer measurement times for the NMR and SEC experiments and to conserve time and material, the number of data points between the measured and apparent viscosities varies. Variation in the shape of the curves at different c_{m0} and n_{eq} stems from a combination of the pseudo-first order kinetics observed for the reaction and the scaling of viscosity with molecular weight. Nonetheless, agreement between the measured and apparent viscosities during the polymerization and within the range of c_{m0} and n_{eq} in the polymer system was reasonable and quantitatively good, considering the difference with how microrheology, NMR, and SEC fundamentally track the polymerization.

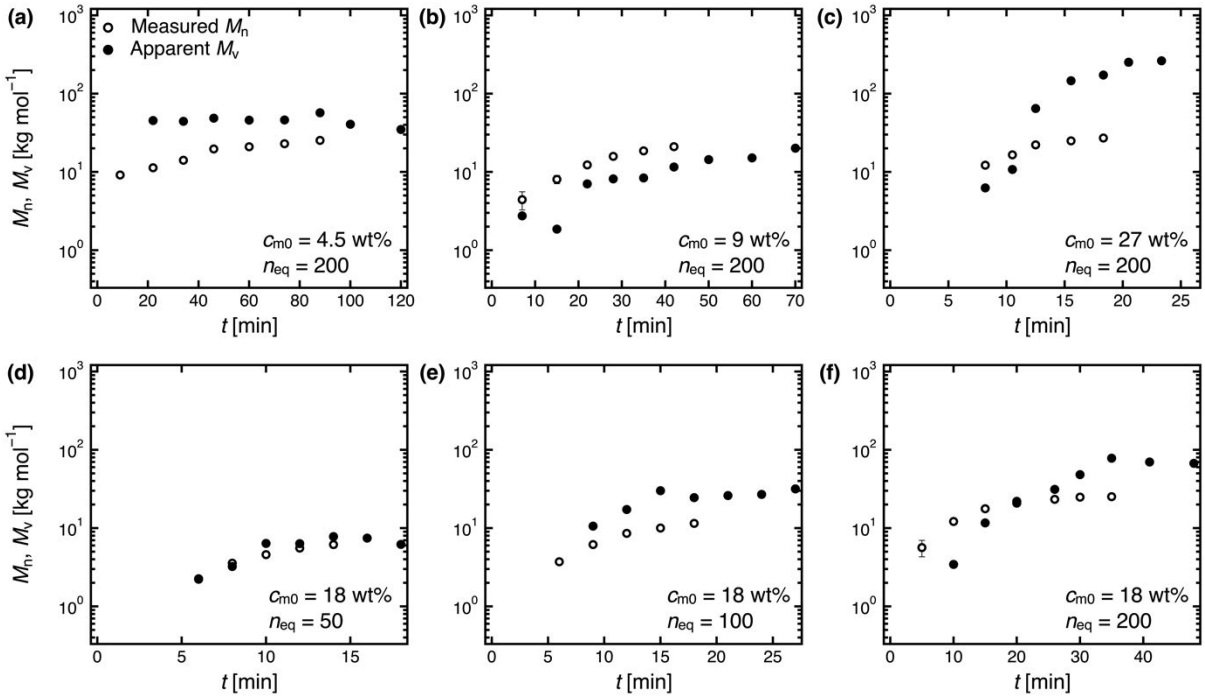

Figure 7. Measured number-average molecular weight, M_n, (empty circles) from size-exclusion chromatography and apparent viscosity-average molecular weight, M_v, (filled circles) estimated from differential dynamic microscopy (DDM)–based microrheology data as functions of polymerization time, t, at various (a–c) initial monomer concentrations, c_{m0}, and (d–f) molar equivalents of monomer relative to the chain transfer agent, n_{eq}. The error bars represent standard deviations of six replicate measurements which, in most cases, are smaller than the data markers themselves.

Similarly, the molecular weight can be estimated from the viscosity measured by DDM microrheology, again using eqs 5-6, and Mark-Houwink constants K and a. In this case, c was expressed in terms of the rate constant, k, (eq S10) through a pseudo-first order rate equation confirmed from the NMR measurements (**Figure S10**). Since the k values from DDM microrheology agree well with those from the conventional NMR and SEC data (**Figure 4**), k from DDM microrheology was used. In this case, DDM microrheology can independently estimate the molecular weight, apart from the calibration which requires measurements of molecular weight using a second analytic technique like SEC. Note that for polymer/solvent pairs with reported Mark-Houwink constants,[28–30] calibration would not be necessary and kinetic microrheology measurements would be completely independent in estimating the molecular weight from the viscosity.

In **Figure 7**, we compare the apparent M_{v} estimated from DDM microrheology and the measured M_{n} from SEC as functions of t at various c_{m0} and n_{eq}. The discrepancy in the number of data points between the measured and apparent values is again due to the experimental constraints mentioned previously. In addition, the discrepancy in molecular weights between the SEC and microrheology measurements may be due to the slightly different average molecular weights estimated by these techniques. This discrepancy becomes more significant at the lower and higher ends of the c_{m0} range. At low c_{m0}, the solution viscosities are close to the solvent viscosity and thereby fall within the measurement resolution. At high c_{m0}, the high polymer concentrations and molecular weights lie beyond the dilute regime and thus the range of validity of the single-point analysis (**Figure S14**). Despite this, good quantitative agreement between the measured and apparent molecular weights was observed, again given the fundamental differences in measurement and analysis between SEC and DDM microrheology, and the simplicity of the equations used to estimate the apparent values.

Using the simple analysis workflow presented here on a model polymer system, DDM microrheology was demonstrated as an accurate alternative to conventional techniques to monitor polymerization because of its high-throughput measurement and analysis. NMR and SEC experiments typically require sample volumes of 100 µL and 700 µL, respectively, with corresponding measurement times per sample of 45 min and 15 min. By contrast, probe microrheology only requires 100 µL samples using multi-well plates, which can be further reduced to < 50 µL using conventional custom-made microscopy sample chambers,[31] and requires only 2-3 min of measurement time. In addition, DDM microrheology analysis does not require user input, making it straightforward and fully automatable; automated extraction of viscosity from one video or image series only takes about 3 min.

Taken together, these results highlight the independence and accuracy of DDM microrheology in estimating the time evolution of molecular weight of a growing polymer using a simple analysis workflow that relates changes in molecular weight to changes in solution viscosity. It is important to emphasize the current limitations of this analysis, specifically, its reliance on dilute conditions, low dispersity, and kinetics that are independent of the molecular weight of the growing polymer. Further studies are therefore necessary to examine the influence of non-dilute concentrations, broad dispersity, and more complex kinetics, and on the ability to extract kinetic information in these cases to determine whether the analysis presented here could be extended to these cases.

4. Conclusions

This work established the use of DDM-based microrheology to monitor the polymerization of a model polymer system. During polymerization, the motion of probe particles embedded in the growing polymer matrix remained diffusive, with a corresponding monotonic increase in solution viscosity with polymerization time. The characteristic rate constant for polymerization extracted from the viscosity measurements was quantitatively consistent with those determined using conventional NMR and SEC techniques. As further validation, an apparent viscosity was estimated from these conventional techniques and an apparent molecular weight from DDM microrheology using the Mark-Houwink and

the single-point Rao-Yaseen equations, which agreed well with the corresponding measured values, but with discrepancies at low polymer concentrations due to the measurement resolution and at high polymer concentrations and molecular weights due to inaccuracy of the single-point analysis beyond the dilute regime. These results demonstrate that DDM microrheology is able to sensitively monitor polymerization through the solution viscosity as an independent alternative to conventional methods. The analysis is simple yet accurate enough to convert the viscosity to the molecular weight of the growing polymer. In addition, the high-throughput, facile, and low-cost measurement and the equally high-throughput, automated, fast, and robust analysis to obtain the viscosity data without the need for user input make DDM microrheology an alternative to techniques conventionally used to monitor polymerization, especially for investigation of large reaction parameter spaces while minimizing material volumes. The ability demonstrated here to use microrheology measurements to extract kinetic parameters and molecular weights could be translated to other controlled radical polymerizations such as atom transfer radical polymerization (ATRP) or nitroxide-mediated polymerization (NMP). More broadly, the technique holds potential to monitor a range of polymerizations and reactions with accompanying changes in rheological behavior, including in situ monitoring of small-volume reactions and high-throughput screening of reaction conditions.

Author Contributions

PSA and CIG are considered co-first authors and contributed equally to the work. PSA synthesized all the polymers and performed NMR and SEC analyses. PSA, CIG, JMU, and YL performed microrheology experiments. CIG developed mathematical methodologies and analyzed data. JMH, RG, MTV, HDM, and MEH initiated and supervised the project. The manuscript was written through the contributions of all authors and all authors have given approval to the final version of the manuscript.

Conflicts of Interest

There are no conflicts to declare.

Acknowledgements

This work was primarily funded by the BASF California Research Alliance (CARA, UCB 052673/SA-10916), with partial support from the BioPACIFIC Materials Innovation Platform (DMR-1933487) and the MRSEC Program of the National Science Foundation under Award No. DMR 1720256 (IRG-3).

References

(1) Frauendorfer, E.; Wolf, A.; Hergeth, W.-D. *Chem. Eng. Technol.* **2010**, *33* (11), 1767–1778.
(2) Florenzano, F. H.; Strelitzki, R.; Reed, W. F. *Macromolecules* **1998**, *31* (21), 7226–7238.
(3) Vega, M. P.; Lima, E. L.; Pinto, J. C. *Polymer* **2001**, *42* (8), 3909–3914.
(4) Colombani, O.; Langelier, O.; Martwong, E.; Castignolles, P. *J. Chem. Educ.* **2011**, *88* (1), 116–121.
(5) Li, B.; Zhang, S.; Tang, L.; Zhou, Q. *Polym J* **2001**, *33* (3), 263–269.
(6) Jessop, J. L. P. *Polymers* **2023**, *15* (18), 3835.
(7) Bachmann, J.; Schmölzer, S.; Ruderer, M. A.; Fruhmann, G.; Hinrichsen, O. *SPE Polymers* **2022**, *3* (1), 41–53.
(8) Pei, D.; Wang, Z.; Peng, Z.; Zhang, J.; Deng, Y.; Han, Y.; Ye, L.; Geng, Y. *Macromolecules* **2020**, *53* (11), 4490–4500.
(9) Schilinsky, P.; Asawapirom, U.; Scherf, U.; Biele, M.; Brabec, C. J. *Chem. Mater.* **2005**, *17* (8), 2175–2180.
(10) Chakrabarty, B.; Ghoshal, A. K.; Purkait, M. K. *Journal of Membrane Science* **2008**, *309* (1–2), 209–221.
(11) Rubinstein, M.; Colby, R. H. *Polymer Physics*; Oxford University Press; 2003.
(12) *Polymer Handbook*, 4th ed.; Brandrup, J., Immergut, E. H., Grulke, E. A., Eds.; John Wiley & Sons, Inc., 2003.
(13) Wagner, H. L. *Journal of Physical and Chemical Reference Data* **1985**, *14* (2), 611–617.
(14) Wagner, H. L. *Journal of Physical and Chemical Reference Data* **1985**, *14* (4), 1101–1106.
(15) Wagner, H. L. *Journal of Physical and Chemical Reference Data* **1987**, *16* (2), 165–173.
(16) Mason, T. G. *Rheologica Acta* **2000**, *39* (4), 371–378.
(17) Furst, E. M.; Squires, T. M. *Microrheology*; Oxford University Press: Oxford, New York, 2017.
(18) Breedveld, V.; Pine, D. J. *Journal of Materials Science* **2003**, *38* (22), 4461–4470.

(19) Schultz, K. M.; Furst, E. M. *Lab Chip* **2011**, *11* (22), 3802–3809.
(20) Bayles, A. V.; Squires, T. M.; Helgeson, M. E. *Rheologica Acta* **2017**, *56* (11), 863–869.
(21) Gu, M.; Luo, Y.; He, Y.; Helgeson, M. E.; Valentine, M. T. *Physical Review E* **2021**, *104* (3), 034610.
(22) Martineau, R. L.; Bayles, A. V.; Hung, C.; Reyes, K. G.; Helgeson, M. E.; Gupta, M. K. *Advanced Biology* **2022**, *6* (1), 2101070.
(23) Cerbino, R.; Giavazzi, F.; Helgeson, M. E. *Journal of Polymer Science* **2022**, *60* (7), 1079–1089.
(24) Perrier, S. *Macromolecules* **2017**, *50* (19), 7433–7447.
(25) Luo, Y.; Gu, M.; Edwards, C. E. R.; Valentine, M. T.; Helgeson, M. E. *Soft Matter* **2022**, *18* (15), 3063–3075.
(26) Billmeyer, F. W. *Textbook of polymer science*, 3rd ed.; Wiley: New York, 1984.
(27) Rao, M. V. R. M.; Yaseen, M. *J. Appl. Polym. Sci.* **1986**, *31* (8), 2501–2508.
(28) Kirkland, J. J.; Rementer, S. W. *Anal. Chem.* **1992**, *64* (8), 904–913.
(29) Holdcroft, S. *Journal of Polymer Science Part B: Polymer Physics* **1991**, *29* (13), 1585–1588.
(30) Gruendling, T.; Junkers, T.; Guilhaus, M.; Barner-Kowollik, C. *Macromolecular Chemistry and Physics* **2010**, *211* (5), 520–528.
(31) McGlynn, J. A.; Wu, N.; Schultz, K. M. *Journal of Applied Physics* **2020**, *127* (20), 201101.